Figure 2 demonstrates serial changes in mean values of the LVIDd, LVIDs, EF, and IVS. From as early as 2 wk postsurgery, LVIDd significantly increased in VO compared with Sham rats. This trend continued up to 12 wk where VO rats exhibited chamber dilatation at diastole that reached 140% of that in Sham rats. The LVIDs in the VO group was significantly increased from 3 wk after shunt compared with that in the Sham group, then continued to increase gradually, and reached 150% of Sham rats after 9 wk. The delay means that the decreasing of cardiac contractility became notable 3 wk after shunt and took at least 9 wk to get worst. The EF in the VO group was increased for the first 2 wk after AV shunt creation and then decreased gradually, and the reduction less than Sham group was first noted at 6 wk. The IVSd in the VO group was slightly thinner compared with that in the Sham group.

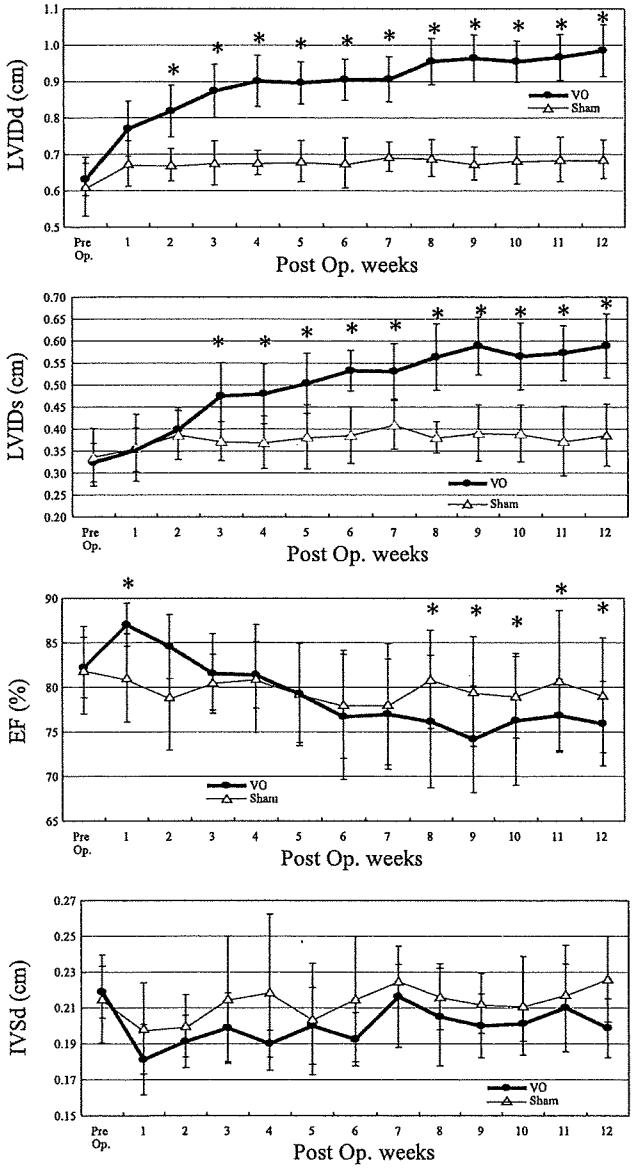

Fig. 2. Serial changes in echocardiographic parameters in VO and Sham rats. The LVIDd, LVIDs, percentage of LV ejection fraction (EF), percentage of LV fractional shortening, and interventricular septal dimensions in diastole (IVSd) are shown. *P 0.05 vs. Sham. As early as 2 wk after the surgery, LVIDd significantly increased in VO compared with Sham rats. This trend continued up to 12 wk where VO rats exhibited chamber dilatation in diastole that reached 140% of that in Sham rats. The LVIDs in the VO group was significantly increased from 3 wk after shunt compared with that in the Sham group, then continued to increase gradually, and reached 150% of that in Sham rats after 9 wk. The EF in the VO group was increased at first 2 wk after arteriovenous shunt but then decreased gradually to become less than Sham group at 6 wk. The IVSd in the VO group was slightly thinner compared with that in the Sham group. Post Op, postoperation of shunt creation or sham procedure.

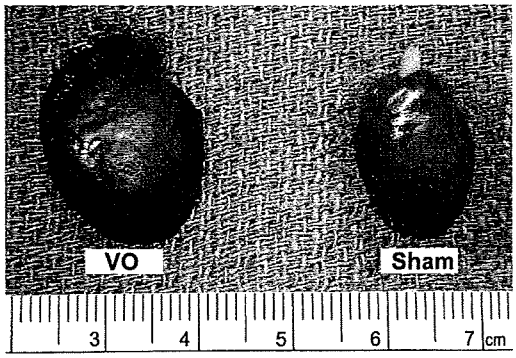

Fig. 3. Whole hearts 3 mo after aortocaval shunt surgery in both VO and Sham rats. The heart in the VO group was markedly enlarged compared with that in the Sham group.

Characterization of Hearts and Lungs

Figure 3 demonstrates the pictures of whole ventricle 3-mo post surgery. The heart in the VO group was remarkably

Table 2. Variables of LV mechanical works and energetics

	Sham		VO		P
ESPVR					
A, mmHg	195	35	134	23	0.003*
B, 1/ml	31.8	24.5	31.6	16.3	0.911
V_0, 10 ^{2} ml/g of LV	7.79	1.11	7.36	1.37	0.601
EDPVR					
A , mmHg	0.20	0.34	0.30	0.26	0.483
B , 1/ml	23.2	9.3	17.1	4.7	0.301
ESP_{mLVV}, mmHg					
Pre-Ca^2 infusion	130	39	98	19	0.039*
Under Ca^2 infusion, 1% $CaCl_2$ 6 ml/h	186	37	127	24	0.003*
ESP_{mLVV}	56	30	29	25	0.045*
$eE_{max,mLVV}$ (baseline), mmHg ml ^{1} g	3,760	1,580	2,395	1,171	0.040*
$\dot{V}O_2$-PVA relation					
Slope, 10 ^{3} l O_2 mmHg ^{1} ml ^{1}	9.70	2.90	7.46	2.63	0.372
$\dot{V}O_2$ intercept, 10 ^{1} l O_2 beat ^{1} g ^{1}	2.77	0.70	2.06	0.89	0.040*
Basal metabolism, l O_2 min ^{1} g ^{1}	16.8	5.9	15.4	4.7	0.123
PVA-independent $\dot{V}O_2$-$eE_{max,mLVV}$ relation					
Slope, O_2 cost of LV contractility, 10 ^{5} l O_2 ml mmHg ^{1} beat ^{1} g ^{2}	6.12	2.14	20.37	6.68	0.047*

Values are means SD; n 7 Sham rats and 7 VO rats. ESPVR, end-systolic pressure-volume relation; EDPVR, end-diastolic pressure-volume relation; ESP_{mLVV}, end-systolic pressure at midrange LV volume (mLVV; see Calculation of PVA); ESP_{mLVV}, (ESP_{mLVV} under Ca^2 infusion) (ESP_{mLVV} pre-Ca^2 infusion); $eE_{max,mLVV}$, equivalent maximal elastance at mLVV; $\dot{V}O_2$, myocardial oxygen consumption per beat; PVA, pressure-volume area. See LV Mechanical and Energetic Studies for ESPVR and EDPVR parameters. V_0 is the unstressed LV volume normalized by LV mass to 1 g. *P 0.05 vs. Sham.

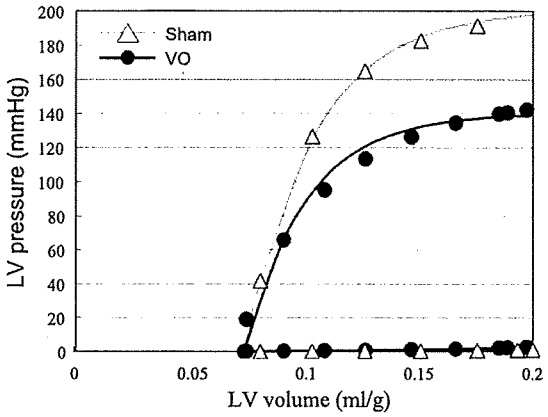

Fig. 4. Representative LV pressure-volume data and the best-fit curves [LV end-systolic pressure (ESP)-volume relation (ESPVR), LV end-diastolic pressure-volume relation (EDPVR)] in each heart for both VO and Sham groups. The LV ESP was markedly decreased in the VO compared with the Sham heart. The LV ESPVR shifted downward but the EDPVR did not shift upward in the VO heart.

enlarged compared with that in the Sham group. Both the LV and RV weights in the VO group were significantly heavier than those in the Sham group (Table 1).

LV Contractility

Summarized data of LV mechanical work and energetics are shown in Table 2.

Figure 4 shows a representative data and best-fit curves of the ESPVR and EDPVR in both VO and Sham group. The LV ESPVR shifted downward, and thus the mean LV ESP_{mLVV} was significantly decreased in the VO group compared with the Sham group (P 0.01; Table 2), although the EDPVR did not shift upward.

Figure 5 shows representative data and best-fit ESPVRs during the Ca^2 infusion of both VO and Sham groups. The contractile response to Ca^2 infusion at a given concentration was smaller in the VO group than that in the Sham group. The mean ESP_{mLVV} in the VO group was significantly smaller (P 0.05) than that in Sham group (Table 2).

LV Energetics

Summarized data of LV energetics are also shown in Table 2.

$\dot{V}O_2$-PVA Relationship

Figure 6 shows each set of representative $\dot{V}O_2$-PVA data and the best-fit $\dot{V}O_2$-PVA linear relations in VO and Sham hearts. The $\dot{V}O_2$ intercept was smaller in this VO heart than in the Sham heart, but the slopes of both $\dot{V}O_2$-PVA relations were similar. The mean $\dot{V}O_2$ intercept was significantly smaller in the VO group than that in the Sham group (Table 2), but the mean slopes of $\dot{V}O_2$-PVA linear relations did not differ significantly between VO and Sham groups (Table 2). Basal metabolism obtained by KCl arrest was unchanged in the VO and Sham groups (Table 2) and thus the significantly smaller $\dot{V}O_2$ intercept in VO group was due to the decreased O_2 consumption associated with Ca^2 handling in E-C coupling.

O_2 Cost of LV Contractility

Figure 7 shows each set of representative PVA-independent $\dot{V}O_2$-$eE_{max,mLVV}$ data and best-fit PVA-independent $\dot{V}O_2$-$eE_{max,mLVV}$ regression lines in both VO and Sham hearts. Each slope of the regression lines denotes the O_2 cost of LV contractility, an index quantifying the $\dot{V}O_2$ for Ca^2 handling per unit change in LV contractility, as mentioned in Data Analysis. The O_2 cost of LV contractility in this VO heart was higher than that in the Sham heart. The mean O_2 cost of LV contractility in the VO group was significantly higher (P 0.05) than that in the Sham group (Table 2).

Immunoblotting of SERCA2a and NCX Normalized to GAPDH

The mean protein level of SERCA2a in VO rat hearts was significantly lower (P 0.01) than that in Sham rat hearts (Fig. 8). We also observed elevated levels (P 0.01) of NCX protein in VO rat hearts (Fig. 9).

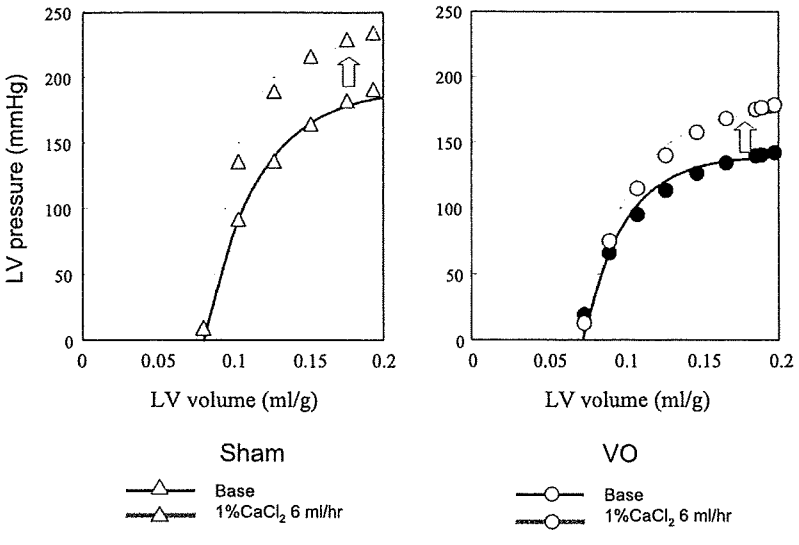

Fig. 5. Representative LV pressure-volume data and ESPVRs under Ca^2 infusion at a rate of 6 ml/h in both hearts from Sham and VO groups. The contractile response to Ca^2 infusion was smaller in the VO heart than that in the Sham heart.

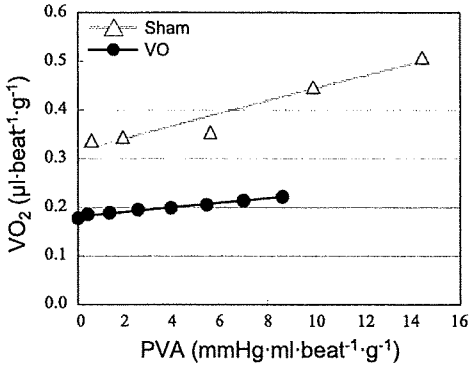

Fig. 6. Representative $\dot{V}O_2$-pressure-volume area (PVA) data and best-fit linear regression lines (the $\dot{V}O_2$-PVA linear relations). The $\dot{V}O_2$ intercept was smaller in the VO heart than in the Sham heart, but the slopes were similar in both VO and Sham hearts.

DISCUSSION

There were several major findings in the VO rats in the present study. LV ESPVR shifted downward, and thus mean ESP_{mLVV} and mean $eE_{max,mLVV}$ (at an mLVV) were significantly decreased compared with those in the Sham rats, indicating systolic dysfunction. The contractile response to Ca^2 infusion (ESP_{mLVV}) was significantly smaller in the VO rats than in the Sham rats. The mean slope of the $\dot{V}O_2$-PVA relation was hardly changed, but the $\dot{V}O_2$ intercept was significantly decreased with unchanged basal metabolism compared with those in the Sham rat, indicating the decreased Ca^2 handling-related $\dot{V}O_2$ at baseline. Finally, the mean slope of the relationship between Ca^2 handling-related $\dot{V}O_2$ and eE_{max} was significantly increased, indicating a less efficient energy utilization in the Ca^2 handling process.

Mechanical Function after AV Shunt

The VO rats created in the present study mainly showed LV systolic dysfunction, whereas diastolic function was almost unchanged. This is compatible with previous studies in a similar VO model in which LV eccentric hypertrophy and systolic dysfunction were apparent, whereas diastolic function and compliance of the ventricle were unchanged or enhanced

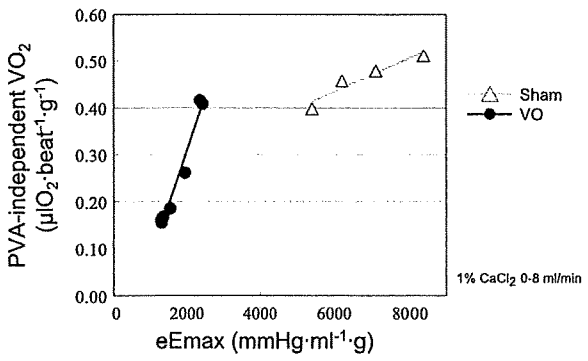

Fig. 7. Representative PVA-independent $\dot{V}O_2$-equivalent maximal elastance (eE_{max}) midrange LV volume data and best-fit regression line (the PVA-independent $\dot{V}O_2$-eE_{max} linear relation; the slope of the relation is the O_2 cost of LV contractility). The O_2 cost of LV contractility in this VO heart was higher than that in the Sham heart.

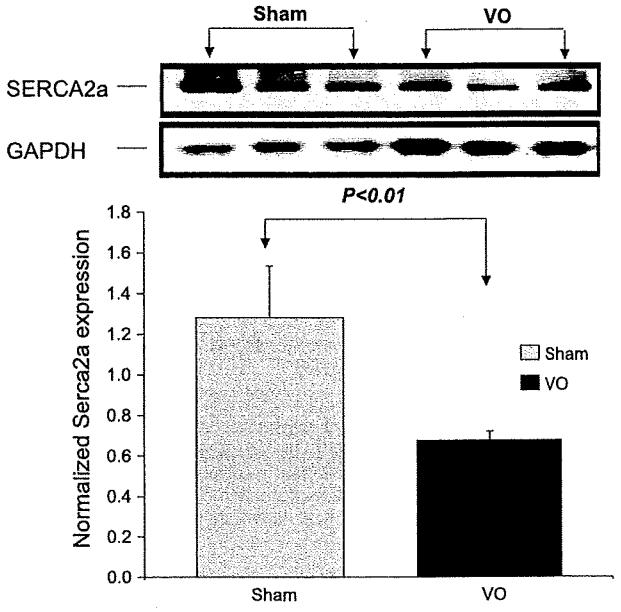

Fig. 8. Immunoblotting of sarco(endo)plasmic reticulum Ca^2 -ATPase 2a (SERCA2a) normalized to GAPDH. The mean protein level of SERCA2a in VO rat hearts was significantly lower (P 0.01) than that in Sham rat hearts.

(4). It is generally accepted that derangement of intracellular Ca^2 handling can play a crucial role in the development of the systolic and diastolic dysfunction accompanying arrhythmia. The mechanism of the LV contractile dysfunction in the present study can be also explained by a derangement of the Ca^2 handling process involved in E-C coupling.

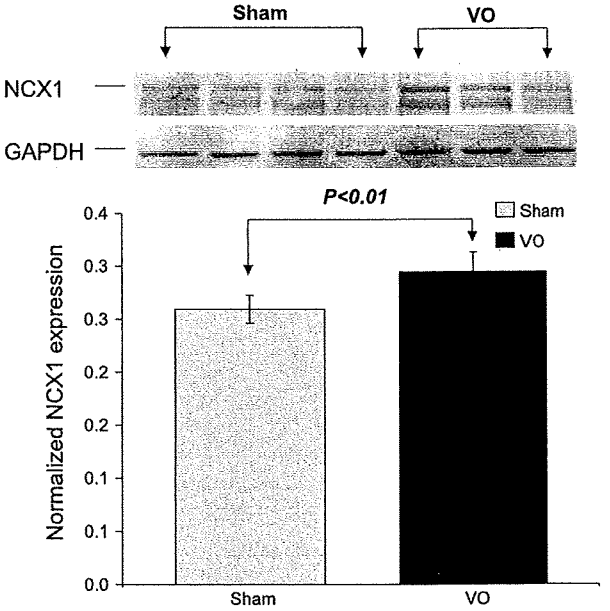

Fig. 9. Immunoblotting of sodium-calcium exchanger (NCX) normalized to GAPDH. The mean protein level of NCX1 in VO rat hearts was significantly higher than that in Sham rat hearts.

Ca^2 Handling in E-C Coupling

We have previously reported that Ca^2 overload in the cytoplasm due to the impairment of the total Ca^2 handling in E-C coupling in the myocardium induced acute cardiac failure (19). The total Ca^2 handling in the myocardium is regulated by transsarcolemmal Ca^2 influx via L-type Ca^2 channel, Ca^2 -induced Ca^2 release via the ryanodine receptor, Ca^2 uptake via the SERCA2a pump, NCX, and Na -K pump coupled to NCX (17). The decreased activity of SERCA2a reduces Ca^2 uptake to the sarcoplasmic reticulum, leading to an increase in cytosolic Ca^2 in diastole and a reduction in Ca^2 release in systole.

In the VO rat, the LV $\dot{V}o_2$-PVA relation has a lower intercept with almost unchanged slope, indicating that total Ca^2 handling O_2 consumption in E-C coupling is decreased under baseline conditions. However, the LV contractility-Ca^2 handling O_2 consumption has a higher slope (O_2 cost of LV contractility), suggesting one possibility that Ca^2 uptake via the SERCA2a pump is suppressed and instead NCX activity is enhanced during inotropic stimulation. Although NCX per se does not consume ATP to remove cytosolic Ca^2 in exchange with influx Na (stoichiometry of 3Na :1Ca^2), the influx Na must be pumped out by Na -K -ATPase with a stoichiometry of 3Na :2K :1ATP, resulting in the net stoichiometry of 1Ca^2 :1ATP (3). On the other hand, SERCA2a removes cytosolic Ca^2 on the basis of a stoichiometry of 2Ca^2 :1ATP. Therefore, the Ca^2 extrusion via NCX leads to twice the increase in energy expenditure compared with Ca^2 uptake by SERCA2a. Thus it seems most likely that the energy wasting in Ca^2 handling is induced mainly by the enhanced NCX activity. In the present study, the expression of the NCX protein was increased in the VO LV tissue. We also reported the same kinds of increased O_2 consumption related to increased NCX activity in a PO hypertrophied rat heart (15). In the failing human heart, a reduction in SERCA2a expression and an increase in NCX expression have been reported (2, 9). This theory was supported by the result in the present study that the SERCA2a protein level was decreased and the NCX protein level was elevated in VO rat hearts. Therefore, in the VO rats, decreased Ca^2 uptake via the SERCA2a pump has impaired cardiac contractility and simultaneously induced energy wasting in E-C coupling.

Another possibility for higher O_2 cost of LV contractility is due to leaky ryanodine receptors. Leaky ryanodine receptors can cause higher cytosolic Ca^2 concentrations in diastole (23), suggesting the possibility for increased energy expenditure by SERCA2a pump. However, the latter hypothesis is unlikely to explain all our findings; indeed, the protein level of SERCA2a in the VO rat hearts was lower than that in the Sham rat hearts, unless NCX1 is upregulated.

A third possibility is due to a lower Ca^2 sensitivity of the myofilament, since ESP_{mLVV} induced by Ca^2 infusion was significantly smaller in the VO rat hearts (see Table 2). However, the increase of PVA-independent $\dot{V}o_2$ was actually larger in the VO rat heart than that in the Sham rat heart under the same protocol for Ca^2 infusion (see Fig. 7). Therefore, the higher O_2 cost of LV contractility seems rather to derive from the larger increase of PVA-independent $\dot{V}o_2$.

Taken together, the possibility that Ca^2 uptake via the SERCA2a pump is suppressed and instead NCX activity is enhanced is the most likely explanation for our findings (15), although further studies including SERCA2a overexpression by gene transfer are needed to verify this possibility.

Chemomechanical Energy Transduction

In the VO hearts, the slope of the $\dot{V}o_2$-PVA relation was almost unchanged or slightly lower compared with that of the Sham heart. The slope of the $\dot{V}o_2$-PVA relation remained unchanged in hypothyroid (11) and diabetic (1) rat hearts, whereas a steeper slope of the $\dot{V}o_2$-PVA relation was reported in hyperthyroid rabbit hearts. It was reported that the slope of the $\dot{V}o_2$-PVA relation was related to the ratio of the myosin isoform component from predominantly V3 to predominantly V1 (i.e., the slope of the $\dot{V}o_2$-PVA relation increases when the V1-to-V3 ratio increases, and the slope of the $\dot{V}o_2$-PVA relation is unchanged when the V1-to-V3 ratio decreases) (6). It was also reported that a progressive decrease in V1 and an increase in V3 were apparent in the LV 8- to 16 wk after AV shunt (21). This report is consistent with the almost unchanged slope of the $\dot{V}o_2$-PVA relation in the VO rats. The slope of $\dot{V}o_2$-PVA relation reflects the ratio of chemomechanical energy transduction efficiency of the contractile machinery. Therefore, in the VO rats, energy wasting is not related to chemomechanical energy transduction.

Conclusion

VO failing rat hearts had a character of marked contractile dysfunction accompanied with inefficient energy utilization especially in E-C coupling.

Present results suggest that restoring the Ca^2 handling process in E-C coupling would improve myocardial contractility in the setting of eccentric cardiac remodeling.

GRANTS

This work was supported in part by National Heart, Lung, and Blood Institute Grants RO1-HL-078691, HL-071763, HL-080498, and HL-083156 (to R. Hajjar) and a grant from Transatlantic Network.

REFERENCES

1. **Abe T, Ohga Y, Tabayashi N, Kobayashi S, Sakata S, Misawa H, Tsuji T, Kohzuki H, Suga H, Taniguchi S, Takaki M.** Left ventricular diastolic dysfunction in type 2 diabetes mellitus model rats. Am J Physiol Heart Circ Physiol 282: H138–H148, 2002.
2. **Arai M, Matsui H, Periasamy M.** Sarcoplasmic reticulum gene expression in cardiac hypertrophy and heart failure. Circ Res 74: 555–564, 1994.
3. **Bers DM.** Calcium fluxes involved in control of cardiac myocyte contraction. Circ Res 87: 275–281, 2000.
4. **Cantor EJ, Babick AP, Vasanji Z, Dhalla NS, Netticadan T.** A comparative serial echocardiographic analysis of cardiac structure and function in rats subjected to pressure or volume overload. J Mol Cell Cardiol 38: 777–786, 2005.
5. **Garcia R, Diebold S.** Simple, rapid, and effective method of producing aortocaval shunts in the rat. Cardiovasc Res 24: 430–432, 1990.
6. **Goto Y, Slinker BK, LeWinter MM.** Decreased contractile efficiency and increased nonmechanical energy cost in hyperthyroid rabbit heart. Relation between O_2 consumption and systolic pressure-volume area or force-time integral. Circ Res 66: 999–1011, 1990.
7. **Hata Y, Sakamoto T, Hosogi S, Ohe T, Suga H, Takaki M.** Linear O_2 use-pressure-volume area relation from curved end-systolic pressure-volume relation of the blood-perfused rat left ventricle. Jpn J Physiol 48: 197–204, 1998.
8. **Lorell BH, Carabello BA.** Left ventricular hypertrophy: pathogenesis, detection, and prognosis. Circulation 102: 470–479, 2000.
9. **Mercadier JJ, Lompre AM, Duc P, Boheler KR, Fraysse JB, Wisnewsky C, Allen PD, Komajda M, Schwartz K.** Altered sarcoplas-

mic reticulum Ca^2 -ATPase gene expression in the human ventricle during end-stage heart failure. J Clin Invest 85: 305–309, 1990.

10. **Miyazaki H, Oka N, Koga A, Ohmura H, Ueda T, Imaizumi T.** Comparison of gene expression profiling in pressure and volume overload-induced myocardial hypertrophies in rats. Hypertens Res 29: 1029–1045, 2006.
11. **Ohga Y, Sakata S, Takenaka C, Abe T, Tsuji T, Taniguchi S, Takaki M.** Cardiac dysfunction in terms of left ventricular mechanical work and energetics in hypothyroid rats. Am J Physiol Heart Circ Physiol 283: H631–H641, 2002.
12. **Sahn DJ, DeMaria A, Kisslo J, Weyman A.** Recommendations regarding quantitation in M-mode echocardiography: results of a survey of echocardiographic measurements. Circulation 58: 1072–1083, 1978.
13. **Sakata S, Lebeche D, Sakata N, Sakata Y, Chemaly ER, Liang LF, Takewa Y, Jeong D, Park WJ, Kawase Y, Hajjar RJ.** Targeted gene transfer increases contractility and decreases oxygen cost of contractility in normal rat hearts. Am J Physiol Heart Circ Physiol 292: H2356–H2363, 2007.
14. **Sakata S, Lebeche D, Sakata N, Sakata Y, Chemaly ER, Liang LF, Tsuji T, Takewa Y, del Monte F, Peluso R, Zsebo K, Jeong D, Park WJ, Kawase Y, Hajjar RJ.** Restoration of mechanical and energetic function in failing aortic-banded rat hearts by gene transfer of calcium cycling proteins. J Mol Cell Cardiol 42: 852–861, 2007.
15. **Shimizu J, Yamashita D, Misawa H, Tohne K, Matsuoka S, Kim B, Takeuchi A, Nakajima-Takenaka C, Takaki MT.** Increased O_2 consumption in excitation-contraction coupling in hypertrophied rat heart slices related to increased Na -Ca^2 exchange activity. Jpn J Physiol 59: 63–74, 2009.
16. **Stromer H, Cittadini A, Szymanska G, Apstein CS, Morgan JP.** Validation of different methods to compare isovolumic cardiac function in isolated hearts of varying sizes. Am J Physiol Heart Circ Physiol 272: H501–H510, 1997.
17. **Takaki M.** Left ventricular mechanoenergetics in small animals. Jpn J Physiol 54: 175–207, 2004.
18. **Takaki M, Kohzuki H, Kawatani Y, Yoshida A, Ishidate H, Suga H.** Sarcoplasmic reticulum Ca^2 pump blockade decreases O_2 use of unloaded contracting rat heart slices: thapsigargin and cyclopiazonic acid. J Mol Cell Cardiol 30: 649–659, 1998.
19. **Tsuji T, Ohga Y, Yoshikawa Y, Sakata S, Abe T, Tabayashi N, Kobayashi S, Kohzuki H, Yoshida KI, Suga H, Kitamura S, Taniguchi S, Takaki M.** Rat cardiac contractile dysfunction induced by Ca^2 overload: possible link to the proteolysis of -fodrin. Am J Physiol Heart Circ Physiol 281: H1286–H1294, 2001.
20. **Tsuji T, Ohga Y, Yoshikawa Y, Sakata S, Kohzuki H, Misawa H, Abe T, Tabayashi N, Kobayashi S, Kitamura S, Taniguchi S, Suga H, Takaki M.** New index for oxygen cost of contractility from curved end-systolic pressure-volume relations in cross-circulated rat hearts. Jpn J Physiol 49: 513–520, 1999.
21. **Wang X, Ren B, Liu S, Sentex E, Tappia PS, Dhalla NS.** Characterization of cardiac hypertrophy and heart failure due to volume overload in the rat. J Appl Physiol 94: 752–763, 2003.
22. **Wang X, Sentex E, Saini HK, Chapman D, Dhalla NS.** Upregulation of -adrenergic receptors in heart failure due to volume overload. Am J Physiol Heart Circ Physiol 289: H151–H159, 2005.
23. **Yano M, Ono K, Ohkusa T, Suetsugu M, Kohno M, Hisaoka T, Kobayashi S, Hisamatsu Y, Yamamoto T, Kohno M, Noguchi N, Takasawa S, Okamoto H, Matsuzaki M.** Altered stoichiometry of FKBP12.6 versus ryanodine receptor as a cause of abnormal Ca^2 leak through ryanodine receptor in heart failure. Circulation 102: 2131–2136, 2000.
24. **Yoshikawa Y, Hagihara H, Ohga Y, Nakajima-Takenaka C, Murata KY, Taniguchi S, Takaki M.** Calpain inhibitor-1 protects the rat heart from ischemia-reperfusion injury: analysis by mechanical work and energetics. Am J Physiol Heart Circ Physiol 288: H1690–H1698, 2005.

J Artif Organs (2009) 12:138–140
DOI 10.1007/s10047-009-0452-9

BRIEF COMMUNICATION

Nozomi Tamura, BS · Takahiko Yamamoto, MS
Hirooki Aoki, PhD · Kohji Koshiji, PhD
Akihiko Homma, PhD · Eisuke Tatsumi, PhD
Yoshiyuki Taenaka, PhD

Investigation of unifying transcutaneous transformer for transmission of energy and information

Abstract When patients are fitted with a totally implantable artificial heart (TAH), they need to be implanted with two additional devices: one for the transmission of energy and one for information. However, this is a cumbersome process that affects the quality of life of the recipient. Therefore, we investigated the use of electromagnetic coupling for the transmission of energy and information and the possibility of unifying two transcutaneous transformers for the simultaneous transmission of energy and information. While unifying the transformers, it is important to suppress the electromagnetic coupling between energy and information transmission. Therefore, we ensured that the electromagnetic fields generated from the transformer windings for the transmissions of information and energy intersected perpendicularly. If the fields are perpendicular, the electromagnetic coupling between the energy and information transmissions will be suppressed significantly. The characteristics of the simultaneous transmission of information and energy using the unified transcutaneous transformer, developed experimentally, were evaluated by changing the number of windings used for the transmission of information. The electromagnetic coupling between the energy and information transmissions was suppressed by determining the direction of the magnetic field. Moreover, the optimum number of transformer windings required for the simultaneous transmission of energy and information was determined. We concluded that the externally coupled transcutaneous transformer unified for the simultaneous transmission of energy and information performed with good transmission characteristics.

Received: March 20, 2008 / Accepted: March 1, 2009

N. Tamura · T. Yamamoto · H. Aoki · K. Koshiji (✉)
Tokyo University of Science, 2641 Yamazaki, Noda, Chiba 278-8510, Japan
Tel. +81-4-7124-1501 ext. 3743; Fax +81-4-7120-1741
e-mail: koshiji@ee.noda.tus.ac.jp

A. Homma · E. Tatsumi · Y. Taenaka
Advanced Medical Engineering Center, National Cardiovascular Center, Research Institute, Suita, Osaka, Japan

Key words Totally implantable artificial heart · Transcutaneous energy transmission system · Transcutaneous information transmission system · Transformer · Quality of life

Introduction

In Japan, heart disease is one of the most common causes of death. At present, heart transplantation is one of the most effective methods for the treatment of a critical cardiac disorder. However, due to the lack of donors, only a few people can receive a heart transplant. To solve this problem, we are researching and developing a totally implantable artificial heart (TAH).

The TAH system must be capable of transmitting energy and information. When patients use the TAH, they need to be implanted with two additional devices for the transmission of energy and information. However, this is a cumbersome process that affects their quality of life (QOL). Therefore, we have investigated the use of electromagnetic coupling for information transmission and the possibility of unifying transcutaneous transformers[1] for the simultaneous transmission of energy and information. In addition, we have evaluated the characteristics of the simultaneous transmission of energy and information by using a unified transcutaneous transformer developed experimentally. The use of the unified transformer ensures that energy and information are transmitted by implanting only one device. As a result, it improves the patient's QOL.

Materials and methods

An energy transmission system for the TAH must have an energy transmission efficiency of 85% or more and a maximum transmission power of 40 W or more (with a rated power of 20 W).[1] Further, an information transmission system must have a transfer rate of 1200 bps or more.[1] This study aims at achieving the above-mentioned targets.

We have investigated the possibility of unifying transformers for the simultaneous transmission of energy and information. However, the unified transformer may result in some interference between energy transmission and information transmission because of the coupling between its windings. Moreover, this interference may cause a reduction in communication integrity. If the interference between the energy and information transmissions is strong, the information transmission circuit might fail.

Therefore, we have attempted reduce the coupling between the energy and information transmissions. In order to avoid interference between the energy and the information transmissions, we have proposed and investigated a transformer whose magnetic fluxes are orthogonal, as shown in Fig. 1. In this transformer (Fig. 1), the magnetic flux induced by the transmission of energy always passes through a toroidal ferrite core; hence, this magnetic flux hardly links with the coil used for the transmission of information. Therefore, the interference between the transmissions of energy and information is reduced. To confirm that the influence from the energy transmission has decreased, we performed the following experiments. When a power of 20 W (rated power) was transmitted (via a 300-kHz rectangular wave), we measured the voltage that was induced in the coil for the transmission of information. Additionally, when a power of 50 W (maximum power) was transmitted, we measured the power that was transmitted to the coil for the transmission of information.

Next, we determined the frequency for the transmission of information. For an implantable data transmission system used for medical treatment, the allocated frequency is from 402 to 405 MHz, as set by the Ministry of Internal Affairs and Communications.[2] Therefore, for this system, we selected a frequency of 405 MHz for the transmission of information.

We have been researching a transcutaneous optical information transmission system (TOITS)[3] for information transmission. The carrier frequency in the TOITS is 76.8 kHz, and we have already achieved a transmission speed of 9600 bps. However, the carrier frequency in the proposed system, 405 MHz, is higher than that of TOITS. Therefore, in the proposed system, it is expected that the transmission speed will be faster than 9600 bps.

Next, it is important to evaluate the inductance and transmittance (S21) of the coil in order to use it at this frequency. If the effective inductance of the coil takes a negative value at 405 MHz, it cannot be used for the transmission of information. The transmittance of the coil is directly related to its transmission characteristics, which show the losses in the coil.

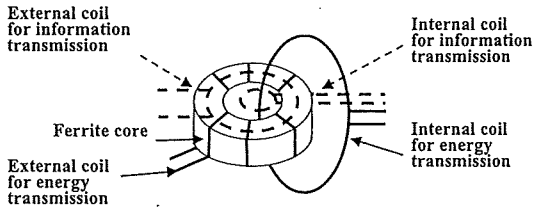

For energy transmission	For information transmission
Size of external coil	Size of external coil
(Toroidal ferrite)	Diameter 30mm
External diameter 38mm	1-turn (0.5mm Copper Wire)
Internal diameter 22mm	
Thickness 14mm	
9-turn (Litz Wire)	
Mn-Zn (Made by FDK)	
Size of internal coil	Size of internal coil
Diameter 40mm	Diameter 10mm
9-turn (Litz Wire)	2-turn (0.5mm Copper Wire)

Fig. 1. Externally coupled transcutaneous transformer for energy and information transmission

Results

The number of turns of the information coils is an important factor for making a transformer. A large number of turns is advantageous for information transmittance because the generated magnetic flux increases. However, many turns in the coil cause self-resonance at low frequency. The inductance of coils takes a negative value above the self-resonance frequency. Hence, it is necessary to determine the optimum number of turns for information transmission.

To confirm whether the external coil developed for testing information transmission is effective, we measured the inductance of the coil at 405 MHz. The results are shown in Fig. 2a. At 405 MHz, a two-turn coil cannot be used

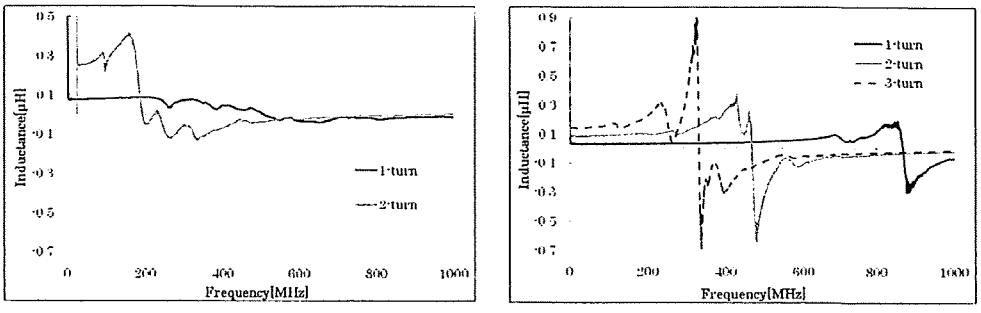

Fig. 2. Inductance of coil for information transmission: **a** inductance of external coil, **b** inductance of internal coil

because its inductance is negative. Therefore, at this frequency a one-turn coil was preferred.

Similarly, the results of the investigation of the internal coil are shown in Fig. 2b. It was found that a one-turn or a two-turn coil can be used for information transmission at 405 MHz but a three-turn coil cannot be used.

Next, the transmittance between the one-turn external coil and the one-turn internal coil was measured by using a network analyzer (Agilent Technologies N5230A, Palo Alto, CA, USA), and it was found to be −10.7 dB at 405 MHz. Similarly, the transmittance between a one-turn external coil and a two-turn internal coil was measured and found to be −9.2 dB at 405 MHz, which is higher than that between the one-turn external coil and a one-turn internal coil. This implies that a one-turn external coil and a two-turn internal coil will have a lower power loss than a one-turn external coil and a one-turn internal coil. Therefore, the coupling between a one-turn external coil and a two-turn internal coil is the optimum coupling strategy for information transmission coils.

For energy transmission, the unified transformer has an energy transmission efficiency of 90% (at a transmission power of 20 W). Additionally, the externally–coupled transcutaneous energy transmission system (ECTETS),[4] which is the energy transmission system for the TAH, has an energy transmission efficiency of 90% (at a transmission power of 20 W), and thus the unified transformer has almost the same energy transmission efficiency as ECTETS.

Next, we performed an experiment to confirm that energy and information could be transmitted simultaneously with the unified transformer. When a power of 20 W was transmitted, the voltage that was induced in the coil for the transmission of information was 1.2 V or less, which could be separated from the information. Additionally, when a power of 50 W was transmitted, the power that was transmitted to the coil for the transmission of information was 0.3 mW or less, which could be separated from the information without significantly reducing the transmission efficiency.

We thus confirmed that the unified transformer could transmit the rated power of 20 W of the TAH and that the spectrum of the received signal for information transmission could be clearly isolated from the energy spectrum. Therefore, we confirmed that energy and information could be transmitted simultaneously with the unified transformer, and the utility of the unified transformer was shown.

Summary

First, we proposed the unification of transcutaneous transformers for the simultaneous transmission of energy and information. Second, we determined the optimum coil coupling for information transmission. Third, we evaluated the transmittance for information transmission. Finally, we confirmed that the unified transformer could transmit energy and information simultaneously. As future work, we will investigate the transmission characteristics of information transmission when the position of the coil changes.

References

1. Tamura N, Yamamoto T, Aoki H, Koshiji K, Homma A, Tatsumi E, Taenaka Y. Transcutaneous energy and information transmission system for a totally implantable artificial heart – unification of externally coupled transcutaneous transformer for energy and information transmission. IEEJ Trans Electron Inform Syst 2008; 128(1):150–151
2. http://www.soumu.go.jp/s-news/2005/050228_1.html. Accessed Oct. 1, 2008
3. Nakaya S, Yamamoto T, Aoki H, Koshiji K, Homma A, Tatsumi E, Taenaka Y. Transcutaneous optical information transmission system for a totally-implantable artificial heart - investigation of crosstalk reduction in full-duplex bidirectional communication using same infrared wavelength. Papers of Technical Meeting on Linear Drives, 2006, IEEJ, LD-06–58
4. Yamamoto T, Koshiji K, Tsukahara K, Tatsumi E, Taenaka Y, Takano H, Shiba K. Externally-coupled transcutaneous energy transmission system for totally implantable artificial hearts – detection of abnormal coupling caused by misalignment and air gap in the ferrite core junction of the transcutaneous transformer. Trans JSMBE 2005;43(2):261–267

Development of An Ultra-Durable Heparin-Free ECMO System

E. Tatsumi

National Cardiovascular Center, Suita, Japan

Summary

We have developed an ultra-durable heparin-free ECMO system with an innovative compact leakless oxygenators and a novel heparin bonding material. The system was evaluated in a series of venoarterial bypass heparin-free ECMO animal experiments using 22 goats. The system could be perfused for over one month (up to three months) successfully. We conclude that our ECMO systems can be applied to wider variety of patients with active bleeding and those with a need of prolonged support.

Introduction

Extracorporeal membrane oxygenation (ECMO) is the only option in treating the patients with life threatening severe respiratory failure. The current system, however, has two major limiting barriers to its extended use. First barrier is poor thromboresistant property of the system that necessitates systemic heparinization, causing serious bleeding complications. Bleeding in sites of canulae insertion, surgery, or injury makes the management of patients extremely difficult. Second barrier is short longevity of the system especially due to plasma leakage from the oxygenator. Microporous gas-exchange membrane, most commonly used in the current membrane oxygenator, easily causes plasma leakage accompanying the loss of hydrophobicity in its protracted use. Therefore, to develop the next-generation ECMO system usable for over a month with minimum or without systemic heparinization is of great clinical significance in terms of opening the door for more liberal application of ECMO to patients with high risk of bleeding or with need of prolonged support.

Recently, we have been developing such next-generation ECMO system, and successfully accomplished over-a-month (up to three months) heparin-free venoarterial bypass ECMO in a series of animal testing.

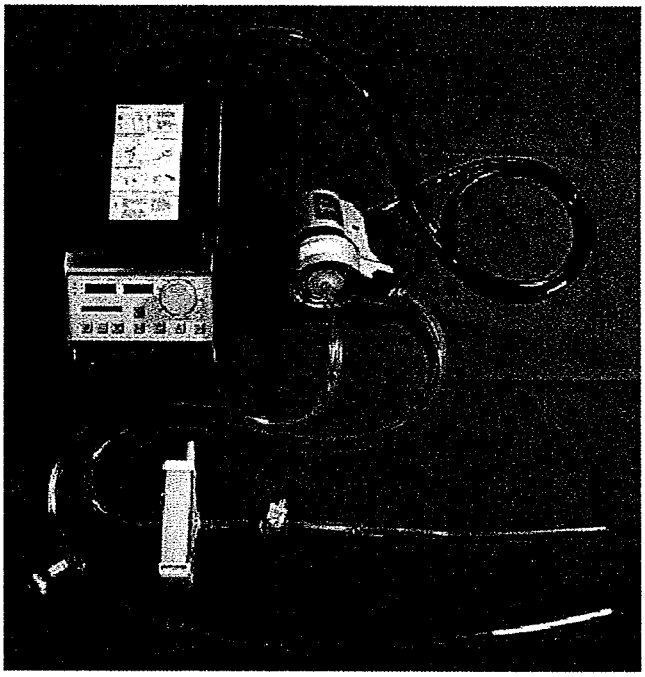

Figure 1 National Cardiovascular Center ECMO system

Materials and Methods

Our ECMO system is composed of a compact oxygenator, a centrifugal blood pump, uptake and return canulae, and connecting tubings (Figure 1). The cube-shaped oxygenator (BioCube-NCVC series, Nipro, Osaka, Japan), consists of a special polyolefin-made hollow fiber membrane in which micropores are blind-ended at the blood contacting surface to create an ultra thin dense layer of less than 0.2 μm thickness, thereby preventing plasma leakage with this unique microstructure [1]. The membrane surface area and the priming volume of the three different sizes of oxygenator are 0.4 m^2 and 45 ml in S-type, 0.8 m^2 and 95 ml in M-type, and 1.3 m^2 and 130 ml in L-type, respectively. As a blood pump, we employed commercially available high-performance centrifugal pump (RotaFlow®, Jostra, Hirrlingen, Germany) that is driven by an outer motor via magnetic coupling and eliminating shaft seal mechanism to obtain long-term durability. The entire blood-contacting surface of the system is treated with a novel powerful heparin bonding material (T-NCVC coating) to impart excellent antithrombogenicity. Detailed feature of the T-NCVC coating was described elsewhere [2]. Differently from the other heparin bonding materials, T-NCVC is endowed with long-term durability and strong antithrombogenicity at the same time.

Chronic animal testing for heparin-free ECMO was carried out in 22 goats weighing from 19 to 60 kg (5 for S-type, 3 for M-type, and 14 for L-type). Under general anesthesia, the uptake and return canulae were inserted into the right cervical vein and the right carotid artery, and the tip of multiple holed uptake canula was anterogradely advanced into the inferior vena cava at the diaphragm position. The ECMO system was connected and positioned on the harness installed on the animal's back, and the venoarterial bypass was started. Systemic anticoagulation was not conducted during

No.	Body weight (kg)	Oxygenator	Bypass Flow (L/min)	Systemic Anticoagulation	Device failure/ Plasma leak	Condition	Duration (days)
1	30	S-type	1.4 - 1.6	no	no	good	67
2	20	S-type	1.4 - 1.6	no	no	good	50
3	19	S-type	1.4 - 1.6	no	no	good	36
4	20	S-type	1.4 - 1.6	no	massive thrombus	good	1*
5	19	S-type	1.4 - 1.6	no	no	good	36
6	41	M-type	2.0 - 2.9	no	no	good	42
7	45	M-type	1.7 - 3.2	no	no	good	65
8	60	M-type	2.9 - 3.3	no	no	good	43
9	58	L-type	2.0 - 2.2	no	no	good	36
10	60	L-type	2.0 - 2.5	no	no	good	60
11	41	L-type	1.7 - 2.4	no	no	good	71
12	59	L-type	1.8 - 2.8	no	no	good	34
13	60	L-type	2.0 - 2.5	no	no	good	39
14	50	L-type	2.0 - 2.8	no	no	good	36
15	54	L-type	1.9 - 2.3	no	no	good	40
16	53	L-type	1.9 - 2.3	no	no	good	35
17	56	L-type	2.4 - 2.6	no	no	good	66
18	64	L-type	2.4 - 2.6	no	no	good	92
19	56	L-type	2.4 - 2.6	no	no	good	36
20	56	L-type	2.4 - 2.6	no	no	good	37
21	50	L-type	2.4 - 2.6	no	no	infection	14*
22	52	L-type	2.4 - 2.6	no	no	good	37

* unexpected termination

Table 1 Summary of heparin-free chronic venoarterial ECMO animal study

the course of perfusion, except for a small dose of heparin at the time of canulae insertion (100 IU/kg intravenous injection) and minute amounts of heparin in the pressure monitoring lines (less than 2 IU/kg/h in total).

Bypass flow was maintained between 1.4 and 3.3 L/min according to the oxygenator size, and an oxygen gas flow to the oxygenator was kept at the same rate as the bypass flow rate. Inflow and outflow blood gases were periodically analyzed to assess the gas-exchange performance. Clotting status was evaluated by measuring activated clotting time (ACT), partial thromboplastin time (APTT), blood heparin concentration, platelet count, fibrinogen, antithrombin III, and clotting factor XIIIa. Hematological and blood chemical studies including plasma free hemoglobin were also performed periodically. At the end of experiment, each system was disassembled for the inspection of thrombus formation, and each animal was subjected to postmortem examination.

Results

Table 1 shows overall results of chronic animal testing. All animals underwent the installation surgery uneventfully. One animal was terminated on day 1 due to massive thrombus formation in the centrifugal blood pump caused by driver failure, and one animal was complicated with infection and terminated on day 14. However, the other 20 animals demonstrated good general condition without any untoward incident till they were electively sacrificed. In those animals, the ECMO system could be continuously perfused without systemic heparinization during the scheduled periods of 34-92 days. Gas-exchange function was kept stable at sufficient level for provided blood flow in each type oxygenator. Plasma leakage was not observed in any case.

The ACT and APTT levels were within normal limits, and the blood heparin concentration was always less than detectable level. No significant change was found

in platelet count, fibrinogen, antithrombin III, and clotting factor XIIIa during the course of experiments. Plasma free hemoglobin and the other hematological and blood chemical data also remained normal.

In postmortem macroscopic and microscopic observations, the hollow fiber bundle of the oxygenator was surprisingly clean against prolonged perfusion with no anticoagulation, although a few clots were found mainly in the marginal area of the inlet and outlet ports. The other parts of the ECMO circuit including the centrifugal pump and canulae were completely free of thrombus.

Conclusions

A durable and thrombo-resistant ECMO system has been developed and evaluated in a series of venoarterial bypass chronic animal testing. The system could be perfused for over one month consistently (up to three months) without systemic heparinization. In Japan, this ECMO system has been already used in clinical settings in the patients with bleeding complications, and demonstrating very good outcomes.

We conclude that our ECMO systems may open the door to wider variety of patients for ECMO, particularly those with active bleeding and those with a need of prolonged support.

References

1. AKASU H, ANAZAWA T, Development of a membrane oxygenator using novel polyolefin hollow fibers with blind-ended micropores, Jpn J Biomater, 8, 141-147, 1990
2. TATSUMI E, NISHINAKA T, TAENAKA Y, KATAGIRI N, OHNISHI H, TAKEWA Y, HOMMA A, TSUKIYA T, KAKUTA Y, SHIOYA K, OSHIKAWA M, SHIRAKAWA Y, MIZUNO T, KAMIMURA T, NAITO H, TAKANO H, SATO M, KASHIWABARA S, TANAKA H, SAKAI K, MATSUDA T, Over two months heparinless venoarterial bypass in goat with a newly developed cardiopulmonary support system treated with novel antithorombogenic material, Proc. 2003 Bioengg Conf, 51, Soslowsky LJ, Skalak TC, Wayne JS, Livesay GA, eds, New York, ASME, pp. 671-673, 2003

空気圧駆動式ウェアラブル全置換型人工心臓システムの開発

—ウェアラブル式空気駆動装置に関する基礎的検討—

Development of wearable pneumatic total artificial heart system
- Fundamental examination of a compact wearable pneumatic drive unit -

○住倉博仁[1], 本間章彦[1], 妙中義之[1], 巽英介[1], 大沼健太郎[1], 赤川英毅[1], 李桓成[1], 武輪能明[1], 水野敏秀[1], 築谷朋典[1], 片桐伸将[1], 角田幸秀[1], 下崎勇生[2], 向林宏[3], 片野一夫[3]
1.国立循環器病センター研究所, 2.株式会社メドウィル, 3.株式会社イワキ
○Hirohito Sumikura, PhD[1], Akihiko Homma, PhD[1], Yoshiyuki Taenaka, MD, PhD[1], Eisuke Tatsumi, MD, PhD[1], Kentaro Ohmuma, PhD[1], Eiki Akagawa, PhD[1], Hwansung Lee, PhD[1], Yoshiaki Takewa, MD, PhD[1], Toshihide Mizuno, DVM, PhD[1], Tomonori Tsukiya, PhD[1], Nobumasa Katagiri, ME[1], Yukihide Kakuta, BE[1], Isao Shimosaki, BE[3], Hiroshi Mukaibayashi, BE[2], Kazuo Katano, BE[2]
1.National Cardiovascular Center, Osaka, Japan., 2.Medwill Technology, Inc., Kanagawa, Japan., 3.IWAKI Co., Ltd., Saitama, Japan.

1. 緒言

補助人工心臓による延命が困難であり、心臓移植以外に有効な治療手段が存在しない末期重症心不全患者に対し、救命・社会復帰を実現するための治療方法が求められている。本研究では、このような不可逆性の両心不全に対する有効な治療手段の一つとして、空気圧駆動式ウェアラブル全置換型人工心臓システムの開発を目的としている。

本システムは左右の空気駆動式ダイアフラム型血液ポンプ、およびシリンダーピストンを使用した空気圧発生機構を有するウェアラブル式小型空気駆動装置から構成される[1]。今回、異なるSD比を有する空気駆動装置を用いて、左右血液ポンプの拍出流量性能評価を行ったので報告する。

2. 方法

ウェアラブル式空気駆動装置(WPD-100)は、ブラシレスDCモータ、クランクシャフト、シリンダーピストン、非円形ギア、空気圧制御弁から構成される。本装置は、シリンダーピストンの往復運動により血液ポンプを駆動する空気圧を発生し、非円形ギアによりSD比を作り出す機構である(Fig.1)。今回、異なる非円形ギアを用いて、35, 40, 44%のSD比を発生可能な駆動装置を作製した。

空気駆動装置の評価実験には、国立循環器病センター製全置換型人工心臓用拍動式左右血液ポンプを用いた。実験は、左右血液ポンプをオーバーフロー型模擬循環回路に接続し、各SD比の空気駆動装置を用いて拍出流量性能評価を行った。また、各駆動装置とも、血液ポンプの駆動状態が完全充満完全駆出駆動するよう適時調整し、実験を行った。

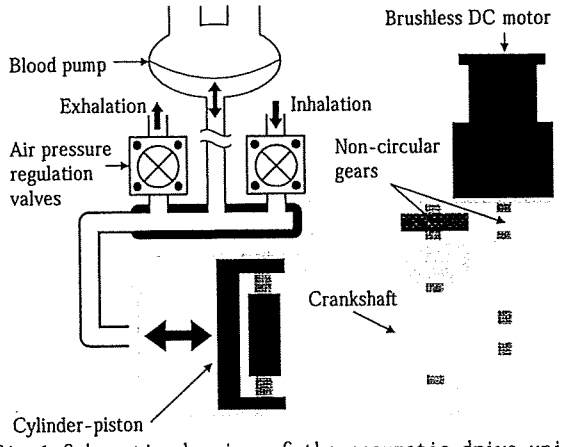

Fig.1 Schematic drawing of the pneumatic drive unit

3. 結果

評価試験の結果をFig.2に示した。左血液ポンプに関しては、前負荷10mmHg、後負荷80 mmHg、拍動数約100bpmにて、SD比35, 40, 44%の最大流量は各々8.5, 8.7, 8.0L/minであった。また、右血液ポンプの最大流量は、前負荷10mmHg、後負荷20 mmHg、拍動数約100bpmにて、10.5, 9.8, 10.3L/minであった。左右血液ポンプ共に、拍動数に対し線形な特性が得られ、異なる後負荷に対しても同様の傾向が確認された。駆動装置の平均消費電力は、左右血液ポンプ共に16～20W程度であり、効率は左血液ポンプが6.5～7.0%、右血液ポンプが約2%であった。

ウェアラブル式空気駆動装置にて、全置換型人工心臓用血液ポンプを十分な適用範囲にて駆動可能なことが確認された。

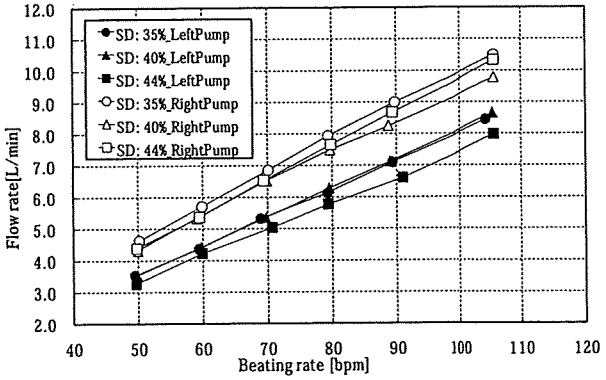

Fig.2 Results of experiment

4. まとめ

本研究ではウェアラブル式小型空気駆動装置のSD比に関し、オーバーフロー型模擬循環回路を用いた基礎的な検討を行い、本装置にて全置換型人工心臓システムに適用可能な拍出流量性能が得られることを確認した。今後、ブラシレスDCモータの制御にてSD比を可変可能な空気駆動装置を開発する予定である。

5. 参考文献

1) Homma A, Taenaka Y, Tatsumi E, Akagawa E, Lee H, Nishinaka T, Takewa Y, Mizuno T, Tsukiya T, Kakuta Y, Katagiri N, Shimosaki I, Hamada S, Mukaibayashi H, Iwaoka W, Development of a compact wearable pneumatic drive unit for a ventricular assist device, J Artif Organs. 2008; 11(4): 182-90.

空気駆動式人工心臓の流量推定に関する研究

Flow Rate Estimation in a Pneumatic Artificial Heart Using the Driveline Air Flow

○大沼健太郎[1]，本間章彦[1]，妙中義之[1]，巽英介[1]，住倉博仁[1]，
赤川英毅[1]，李桓成[1]，武輪能明[1]，水野敏秀[1]，築谷朋典[1]，片桐伸将[1]，角田幸秀[1]，
下崎勇生[2]，向林宏[3]，片野一夫[3]
1．国立循環器病センター研究所，　2．株式会社メドウィル，　3．株式会社イワキ
○Kentaro Ohnuma[1], Akihiko Homma[1], Yoshiyuki Taenaka[1], Eisuke Tatsumi[1], Hirohito Sumikura[1],
Eiki Akagawa[1], Hwansung Lee[1], Yoshiaki Takewa[1], Toshihide Mizuno[1], Tomonori Tsukiya[1], Nobumasa Katagiri[1],
Yukihide Kakuta[1], Isao Shimosaki[2], Hiroshi Mukaibayashi[3], Kazuo Katano[3]
1. National Cardiovascular Center Research Institute, 2. Medwill Tecnology Inc., 3. IWAKI CO., LTD.

1．緒言

心臓移植がドナー不足により長い待機期間を要する現時点において、補助人工心臓(Ventricular Assist Device, 以下 VAD)は、重症心不全患者の救命に重要な治療機器となっている。VAD による長期循環補助においてポンプ拍出量を把握することは重要であるが、専用の流量計の組み込みは、システムが複雑で高価となるなどの問題を有する。

そこで、本研究では本邦で主に使用されている空気駆動式の東洋紡社製血液ポンプとわれわれのグループで開発中のウェアラブル式空気駆動装置[(1)]を用いて、空気駆動用エアホース(ドライブライン)に組み込んだ熱式質量流量センサより得られる空気流量を利用することで、簡易に血液ポンプの分時拍出量を推定のための基礎的な検討を行ったので報告する。

2．方法

本研究で対象とした VAD は容積型ポンプであるため、ドライブラインの空気流量と血液ポンプの瞬時拍出量には相関性があると考えられた。そこで基礎検討として、オーバーフロー型模擬循環回路によるポンプ駆動実験を行い、駆出方向の空気流量と超音波流量計により計測した駆出方向の瞬時流量との関係について回帰分析を行った。具体的には、東洋紡社製血液ポンプと開発中のウェアラブル式空気駆動装置を市販の熱式質量流量センサを組み込んだドライブラインを介して接続し、循環流体は水道水として駆動実験を行った。駆動条件は SD 比 35%、前負荷 10 mmHg を一定とし、拍動数を 60, 70, 80, 90, 100 bppm、後負荷 60, 80 100 mmHg として、完全充満・完全駆出駆動した際の空気流量とポンプ拍出量を計測した。

3．結果

計測結果の一例として、拍動数 80 bpm、後負荷 100 mmHg における血液ポンプの瞬時流量波形とドライブラインの空気流量波形を Fig. 1 に示した。このとき、1 分間の各流量波形について駆出方向の相関関係を Fig. 2 に示した。同様にして、各条件ごとに 1 分間の計測データについて位相補正を施して回帰分析を行った結果、駆出方向の瞬時拍出量と駆出方向空気流量は決定

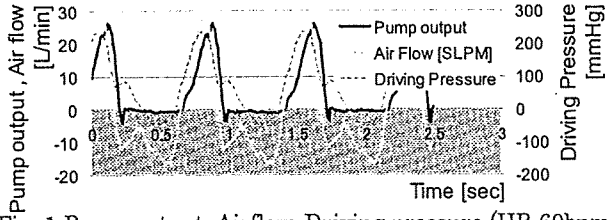

Fig. 1 Pump output, Airflow, Driving pressure (HR 60bpm, Afterload 100mmHg)

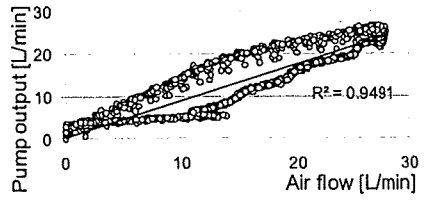

Fig. 2 Correlation between pump output and air flow

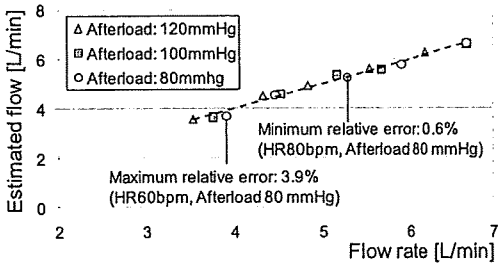

Fig. 3 Flow rate of Toyobo blood pump vs. Estimated flow

係数 0.90~0.98 で強い正の相関が認められた。

良好な相関が得られたことから、模擬循環回路によるポンプ駆動において得られた駆出方向の空気流量を用いて、最小自乗近似にて求めた簡易な推定式から血液ポンプの分時拍出量推定を行った。その際、ポンプ流量の逆流分を考慮して、推定式に駆動実験での逆流量に基づいた補正項を設けた。各駆動条件における分時拍出量と推定結果を Fig. 3 に示した。このとき、最小誤差 0.6%(拍動数 60 bpm、後負荷 80mmHg)、最大誤差 3.9%(拍動数 80 bpm、後負荷 80mmHg)で推定が可能であった。

4．まとめ

本研究では、空気駆動式血液ポンプを対象にドライブラインの空気流量を利用した拍出量推定について基礎検討を行い、駆出方向の瞬時流量と空気流量波形の間に良好な相関が認められた。また、空気流量を利用して簡易な推定式から血液ポンプの分時拍出量推定を行い、最小誤差 0.6%、最大誤差 3.9%で推定値が得られたことから、本手法の有用性が示された。

今後、流体の粘性や循環系のコンプライアンスの影響、生体に装着した際の負荷が動的に変動する条件などを考慮して、さらに検討を進める予定である。

5．参考文献

(1) Akihiko Homma, Yoshiyuki Taenaka, Eisuke Tatsumi, *et al.* , Development of a compact wearable pneumatic drive unit for a ventricular assist device, J Artif Organs. 2008; 11(4): 182-90.

呼　吸　28巻7号　別刷

平成21年7月
レスピレーション リサーチ ファンデーション

解　説　基　礎

人工肺
—研究開発と臨床応用の現況—

巽　英介

要　旨　人工肺は，生体肺の最も重要な機能であるガス交換(呼吸機能)を肩代わりする装置で，主として開心術時の補助手段である人工心肺装置として用いられる。人工肺には，基本となるガス交換性能に加えて，耐久性や血液適合性，操作性・安全性などが求められる。現在わが国で用いられている人工肺のほぼすべてが，多孔質中空糸膜を用いた膜型人工肺である。開心術用の人工肺が十分な性能を有するにいたった一方で，近年人工肺を呼吸循環補助に応用する例が増加しつつあり，長期使用が可能な人工肺や抗血栓性に優れた人工肺，さらに血液ポンプと一体化した人工肺やカテーテル型人工肺など，次世代型の人工肺を目指した研究開発が活発に行われている。このような補助循環の分野を対象とした高性能人工肺の開発は，多くの重症患者の救命に繋がるものと考えられ，今後の開発研究の一層の推進と臨床応用の発展が期待される。

巽 英介：人工肺—研究開発と臨床応用の現況—．呼吸 28(7)：708—714，2009
キーワード：人工肺，開心術，体外循環，人工心肺装置，ECMO

はじめに

「人工肺」は，生体肺の呼吸機能，即ち血液に酸素を添加し血液から炭酸ガスを除去するガス交換の働きを肩代わりする装置である。主として心臓手術(開心術)時の「人工心肺装置」の一部として用いられ，多くの開心術は人工肺なしでは行い得ない。このような働きをする人工肺に対しては，ガス交換性能のみならず耐久性や血液適合性，操作性・安全性などが求められ，様々な材料的・構造的ノウハウが詰め込まれている。本稿では，人工肺の研究開発と臨床応用について，現況を中心に概説する。

Artificial lungs : current state of research and development and clinical use
国立循環器病センター研究所人工臓器部
Eisuke Tatsumi
National Cardiovascular Center Research Institute, Department of Artificial Organs, Osaka 565-8565, Japan

Ⅰ．開心術における人工心肺装置の役割

日本では毎年3万例以上，米国では毎年10万例以上の開心術が行われている。開心術の病院死亡率は一般的な待機手術では1％以下，緊急手術や重症例を含めても3〜4％程度であり，今日の開心術は広く定着した日常的な医療といえるが，その最大の契機となったのが人工心肺装置の登場である。人工心肺装置が生体の心臓と肺の機能を肩代わりすることで，心臓内部を血液が殆ど流れない状態にしたり，心臓の動きをいったん停止させることが可能となり，これによって開心術が今日のように短時間で安全に行えるようになった。

人工心肺装置(図1)は，全身から血液が還ってくる大静脈と心臓が全身に向けて血液を送り出す大動脈の間で並列して患者と接続され，血液は生体の心臓と肺をバイパスする形で装置内を灌流する(体外循環)。人工心肺装置は，大

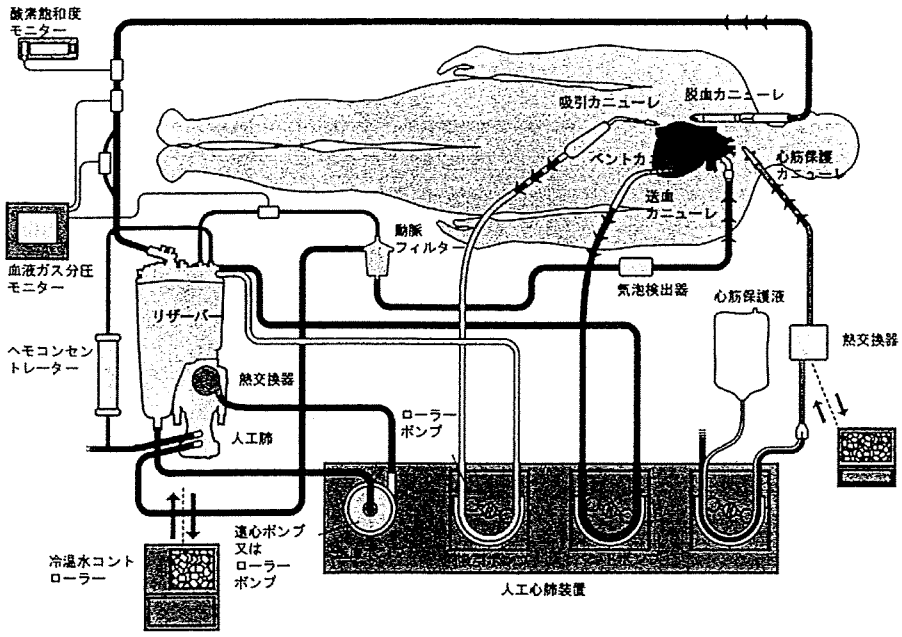

図1　人工心肺装置

静脈に留置した脱血管を通して血液を装置に流れ込ませる脱血ライン，術野に貯まった血液を回収する吸引ライン，脱血した血液や吸引血を一時的に貯める貯血槽，ガス交換を行う人工肺，ガス交換後の血液を送血するための血液ポンプ，送血血液中の微小気泡や微小凝血塊を取り除く動脈フィルター，そして動脈に留置した送血管まで血液を導く送血ラインなどで構成される。そして，これらの構成パーツの中で中心的な役割を果たしているのが，ガス交換機能を担う人工肺である。

Ⅱ．人工肺開発の歴史

人工肺開発の歴史をたどると，外科医の Gibbon が 1937 年に世界ではじめて動物の呼吸と循環を代行する実験に成功したことにさかのぼる。その後「スクリーン型」という人工肺を完成させ，20 年間におよぶ研究を経て，1953 年に最初の臨床応用が行われた[1]。やがて「スクリーン型」は「フィルム型」へと進化し，さらに高性能・高耐久性を有する回転円板型人工肺(図 2)が開発され，1960 年代に広く普及した。これらのタイプはいずれも，金属表面に血液の薄膜を形成して酸素ガスとの間でガス交換を行うという機構であった。その後，ディスポーザブル化が可能な気泡型人工肺が出現し，1970 年代を代表する人工肺となった。これは，血液と酸素ガスを直接混ぜ合わせて十分にガス交換を行った後に，血液中の気泡を取り除いて全身に返すという機構のものである。ただし，気泡型人工肺は，

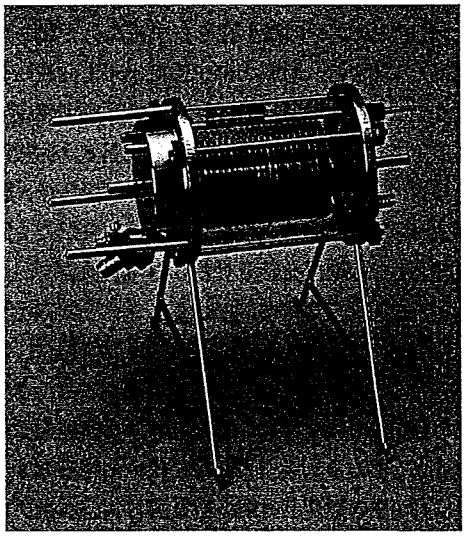

図2　開発初期の回転円板型人工肺(Pempco Kay-Cross 型，1956 年)

ガス交換効率は非常に良好であったが，その一方で血液の凝固反応や炎症反応が著しく亢進するという短所があった。

一方，1944 年に Kolff が，透析患者の血液が人工腎のセロファン膜を介して酸素加される現象に気付いて人工肺への応用を試みたものが，現在主に用いられている「膜型人工肺」の開発の端緒である[2]。血液と酸素が直接接触しない膜型人工肺は「生理的人工肺」として期待されたが，技術的困難も多く，1968 年になってようやくシリコンラバー膜を用いたものが製品化された。しかし，当初は気泡型に比べてガス交換性能が劣り，また操作が煩雑でコストダウ

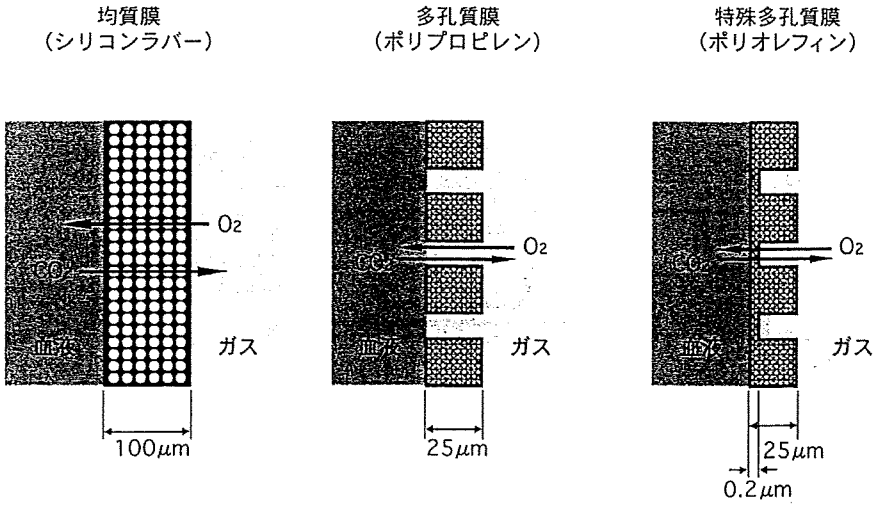

図3 膜型人工肺に用いられるガス交換膜の種類

ンが困難など，まだまだ多くの問題をかかえていた。

膜型人工肺の革新技術となったのが，1979年にわが国の研究グループによって開発された「多孔質中空糸膜」である[3]。サブミクロンの微小孔を有する高分子膜を用いた多孔質膜人工肺では，材料の疎水性によって血液は微小孔から漏れ出ない(ただし長期間の使用では，蛋白吸着・疎水性低下によって血漿成分がガス相に漏れ出す「血漿漏出」が起こる)。この人工肺は，従来のシリコンラバー膜型肺と気泡型肺の利点を併せもつものとして，またたく間に汎用人工肺としての地位を確立した。

Ⅲ. 現在の膜型人工肺の基本構造

現在わが国で用いられている人工肺は「膜型人工肺」がほぼ100％を占める。膜型人工肺に用いられるガス交換膜としては，シリコンラバー製の均質膜およびポリプロピレン製を中心とする多孔質膜があり，特殊な多孔質膜として薄い均質層をもつ非対称膜がある(図3)。シリコンラバー膜の膜厚は100μm程度で，血液と酸素ガスは直接接触せず，膜を介する拡散によってガス交換が行われる。一方，多孔質膜の膜厚は20～30μmで，孔径0.03～0.07μmの多数の微小孔が膜を貫通して内外面で開口し，血液接触面において微小な血液/ガス界面を形成してガス交換が行われる。

膜モジュールの形態としては平膜と中空糸膜があるが，現在はすべて中空糸膜である。直径200～300μmの中空糸膜は，それ自体が支持組織となるため設計の自由度も高く，体積当たりのガス交換膜面積が多く人工肺内部の血流状態の制御性も良好であるなど，多くの利点を有している。開発当初は中空糸の内側を血液が流れる「内部灌流方式」であったが，現在は中空糸の外側を血液が流れる「外部灌流方式」が主流となっている。外部灌流方式のほうが人工肺内部の圧損失が低く，また設計の工夫によってより効率的なガス交換性能が得られるからである。

中空糸は束ねたり編んだりしてバンドル化されて，人工肺のケーシングに収容される(図4)。バンドルの両端はポッティング剤という接着剤で固められる。バンドル化に際しては，内部の血流状態を最適化することが重要であり，中空糸をできるだけ均等な間隔で，しかも適当な密度(充塡率)で配置する必要がある。中空糸間の距離が不均一だと流れにチャンネリングが生じてガス交換効率は低下し，逆に密に束ね過ぎると圧力損失が大きくなって血球破壊や血液の鬱滞を招く。血液が効率的に混ざり合うような血流状態の確保も重要であり，これらの要因を勘案した最適な充塡率は，経験的に40～45％程度とされている。

Ⅳ. 人工肺の臨床使用の現状と動向

わが国における最近の人工肺の使用状況については，矢野経済研究所が行っている出荷数ベースの調査[4]によると，2006年度の総出荷数は43,866個で，このうち一般開心術用が39,116個，経皮的心肺補助(PCPS)や呼吸補助(ECMO)など補助循環用が4,750個となっている。開心術用人工肺の使用数は2000年頃までは毎年1,500個前後のコンスタントな増加(年間増加率5～6％)を示してきたが，以後は明らかな頭打ち傾向を示している。これには，冠動脈ステントなどの経皮的冠動脈インターベンション(PCI)の普及，そして体外循環を使わない冠動脈バイパス術(off-

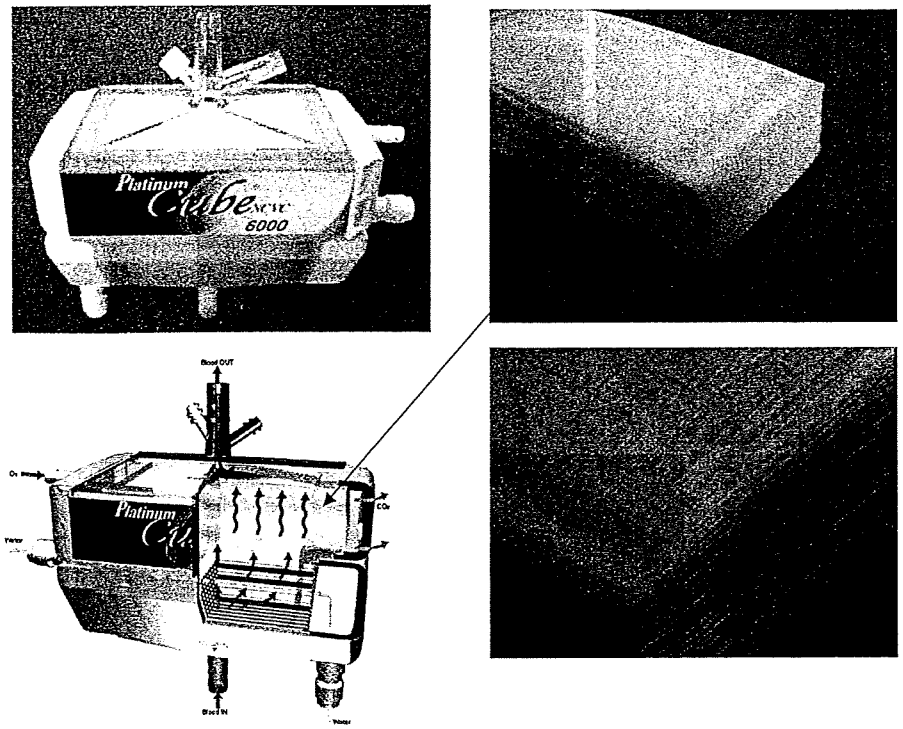

図4　ガス交換膜(中空糸バンドル)を内蔵した膜型人工肺

pump CABG)症例の増加などが大きく影響しているものと考えられる[5]。

一方，補助循環症例への使用数も2002年頃までは毎年10～20％前後の顕著な増加を示してきたが，最近は増加傾向が鈍りつつある。膜型人工肺研究会が毎年行っているアンケート調査[6]によると，2007年のECMOの施行症例数は，回答のあった75施設の合計で465例となっている。また，PCPS研究会が行った全国集計調査(回答施設148施設)では[7]，PCPS症例数は年間700～800例に達し，臨床成績も明らかに向上してきている。世界的な集計としては，米国Michigan大学を拠点とするExtracorporeal Life Support Organization(ELSO)が毎年全世界の主要なECMOセンターにおける症例の登録・解析を行っている。2008年6月の報告[8]によると，調査が開始された1987年以降の累積症例数は37,717例に達し，離脱率は75％，生存率は63％となっている。また，123施設から回答を得た2007年の症例数は2,290例に上っており，現在も増加傾向にある。

Ⅴ．補助循環を目的とした研究開発の動向

人工肺は，現在では開心術用の使用においてほぼ十分な性能を有するにいたったといえる。その一方で，補助循環への応用が進むとともに，さらなる小型化や，長期耐久性，高い抗血栓性などが求められるようになり，ガス交換膜材質の開発・改良や回路への抗血栓性付与などに重点をおいた研究開発が続けられている。

ポリプロピレン製多孔質膜では，長期間使用時に疎水性が失われて微小孔からの血漿漏出を生じるため，数日程度の使用が限界である。また，血液―ガス界面を有するために，微小気泡の混入や生体の炎症反応・血液凝固反応を亢進させる。この問題を克服するガス交換膜として，種々の複合膜が検討されている。シリコンやシリカの微小孔への充填，血液接触面へのフッ素コーティングなど，ガス交換性能を可及的維持し得る材料で多孔質膜の微小孔を封じる試みが行われ，シリコンで表面コーティングを施した多孔質膜は既に実用化されている[9]。また，単一素材のガス交換膜として，シリコン中空糸膜[10]や含フッ素ポリイミド中空糸膜[11]などが開発されており，さらに多孔質膜の血液接触面に極薄の緻密層を形成したポリメチルペンテン製の非対称膜(図5)も製品化されている[12]。これらのガス交換膜では血液相とガス相を遮断して血漿漏出を防止しているが，耐久性のみならず血液適合性の面からも大きな利点である。

一方，現行の人工肺は抗血栓性に乏しく，使用に際して生体由来抗凝血薬である「ヘパリン」を患者に投与する必要がある。開心術等の短時間使用であれば問題は少ないが，補助循環等の長期使用においては，出血傾向を惹起してリスクが増大する。ヘパリン投与量の低減を目的として人工

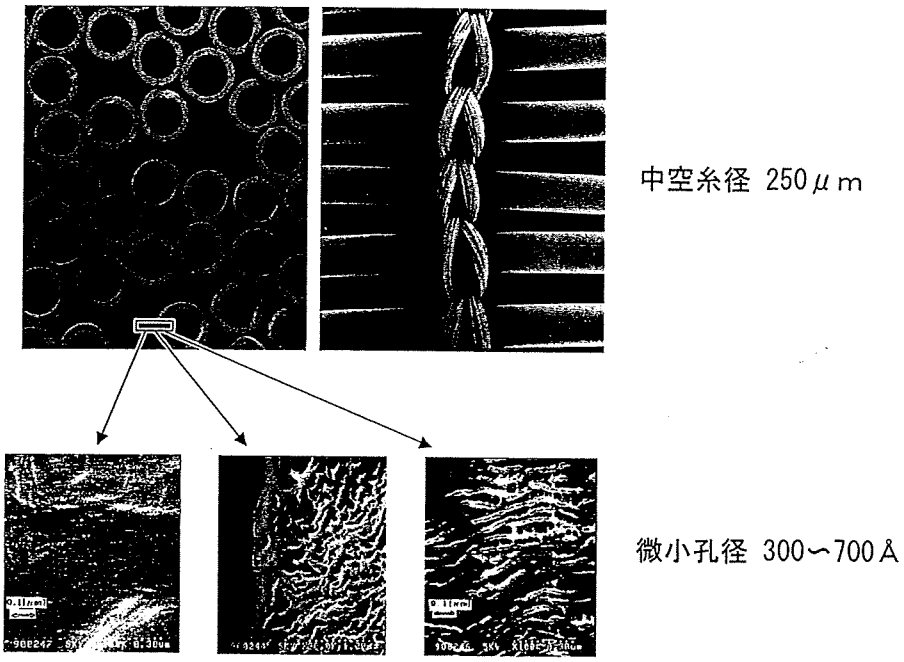

図5 ポリメチルペンテン製の非対称ガス交換膜

肺に抗血栓性を付与するための様々な試みが行われてきたが，現在主流となっているのは，血液接触面に化学的にヘパリンを導入(徐放または固定化)する方法である。このアプローチによっても，ヘパリン投与量は減量できても完全な不要化は困難であるが，国立循環器病センターで開発された人工肺[12)13)]およびヘパリンコーティング法[14)]を用いたECMOシステムは，慢性動物実験でヘパリン投与を行うことなく3カ月以上の連続使用を達成し[15)]，臨床例においても出血を合併する重症患者などに用いられて優れた成績を収めている。

Ⅵ. 新しいシステムの開発と臨床応用

通常のECMOやPCPSでは，循環補助であれば静脈—動脈(V-A)バイパス，呼吸補助であればV-Aバイパスまたは静脈—静脈(V-V)バイパス方式で施行されるため，送血用の血液ポンプが必要となる。一方，動脈—静脈(A-V)バイパス方式であれば，二酸化炭素除去に機能は限定されるが(arterio-venous CO_2 removal：$AVCO_2R$)，バイパス血流量が過大でなければ動脈圧で人工肺を灌流できる可能性があり，血液ポンプをなくすことができる。Novalung GmbH社は，このA-Vバイパス方式ポンプレスECMOシステムを「iLA」という名前で製品化しており，重症肺炎や外傷性ARDS，肺移植へのブリッジなどを中心に，欧州で既に1,500例以上の症例に対して用いられている[16)]。

人工肺では，血流が鬱滞しやすい部位で血栓が形成されやすく，血流路や血液接触面積なども含めた装置のデザインが重要である。このような観点から，血液ポンプと人工肺を一体化させて装置内部の血流状態を最適化し，同時にガス交換性能の最大化と装置全体の小型化を図るという開発アプローチが考えられる[17)]。この概念は国立循環器病センターで最初に提案され，設計・試作が行われた(図6)。現在では，Helmholtz-Instituteの「HEXMO」[18)]やEnsion社の「pCAS」[19)]など，同様のコンセプトに基づく装置が製品化を目指して開発されつつある。

一方，体内埋込み型人工肺に関しては，Michigan大学およびMC3社によって，胸腔内埋込みを目指し，肺動脈—左心房間に血液ポンプなしで接続できるようにデザインされた低圧損失人工肺「BioLung」の開発が進められている[20)]。埋込み型人工肺の一種である静脈内留置型人工肺「IVOX」は，患者の大静脈内に中空糸束を直接挿入することでハウジングや灌流装置の不要化を目指した装置であり，1987年に最初に提唱された[21)]。臨床試験も行われたが，様々な問題点により1994年に開発は中止された。しかしながら，その後もこのコンセプトは引き継がれて，新たな工夫を加えた装置開発が継続されている。Pittsburgh大学の「Hattlerカテーテル」は，静脈内に留置した中空糸束の中心に細長いバルーンを配し，これを拍動させることで高いガス交換性能を得ようとするものである[22)]。

以上のような機器開発を中心とする研究に加えて，以前から継続的に行われている液体呼吸関係の研究についても，